CHAPTER 7

Accuracy of motor axon regeneration across autograft, single lumen and multichannel poly(lactic-co-glycolic acid) (PLGA) nerve tubes

Godard C.W. de Ruiter [1,3,5], Michael J. Moore [2], Martijn J.A. Malessy [5], Robert J. Spinner [3], Eric J. Sorenson [4], Bradford L. Currier [2], Michael J. Yaszemski [2], Anthony J. Windebank [1]

[1] Laboratory for Molecular Neuroscience, Mayo Clinic, Rochester MN, USA
[2] Laboratory for Biomedical Engineering, Mayo Clinic, Rochester MN, USA
[3] Department of Neurologic Surgery, Mayo Clinic, Rochester MN, USA
[4] Department of Clinical Neurophysiology, Mayo Clinic, Rochester MN, USA
[5] Department of Neurosurgery, Leiden University Medical Center, the Netherlands

Published in Neurosurgery, July 2008, Volume 63 (1); 144-153 (comments 153-155)

ABSTRACT

Background The accuracy of motor axon regeneration becomes an important issue in the development of a nerve tube for motor nerve repair. Dispersion of regeneration across the nerve tube may lead to misdirection and polyinnervation. In this study, we present a series of methods to investigate the accuracy of regeneration, which we used to compare regeneration across autografts and single lumen poly(lactic-co glycolic acid) (PLGA) nerve tubes. We also present the concept of the multichannel nerve tube that may limit dispersion by separately guiding groups of regenerating axons.

Methods Accuracy of motor axon regeneration across autograft, single lumen and multichannel poly(lactic co-glycolic acid) (PLGA) nerve tubes was investigated in a 1-cm gap of the rat sciatic nerve model 8 weeks after repair with simultaneous and sequential retrograde tracing. Simultaneous tracing of the tibial and peroneal nerve was performed to quantify axonal dispersion. Sequential tracing of the peroneal nerve was performed to quantify the percentage correctly directed peroneal motoneurons. In addition, quantitative results of regeneration were determined from compound muscle action potential recordings, nerve and muscle morphometry.

Results More motoneurons were found to have double projections to both the tibial and peroneal nerve after single lumen PLGA nerve tube (21.4%) than after autograft repair (5.9%). Multichannel PLGA nerve tube repair slightly reduced this percentage (16.9%), although not significantly. The direction of regeneration was nonspecific after all types of repair. Quantitative results of regeneration were similar after single lumen and multi-channel PLGA nerve tube repair, despite the smaller total cross-sectional channel area for multichannel nerve tubes. Overall quantitative results of regeneration were superior after autograft repair.

Conclusions Dispersion of regenerating axons across single lumen nerve tubes may limit the results in the repair of motor nerves innervating different distal targets. Multichannel nerve tubes proved to be a promising alternative, but need to be further optimized for possible future clinical application.

INTRODUCTION

Single lumen or hollow nerve tubes have been developed as alternative to nerve gap repair with an autologous nerve graft (**Chapter 5**). The advantage of repair with a nerve tube is the unlimited, right-of-the-shelf availability in a range of sizes without additional donor-site morbidity. The first biodegradable nerve tubes are now available for clinical use [1]. These nerve tubes are mainly used in the repair of small sensory nerves, such as digital nerve lesions with gaps up to 3 cm [2], and have recently been used in the repair of larger motor nerves [3, 4]. Single lumen nerve tube repair, however, may lead to inappropriate target reinnervation by the dispersion of regenerating axons across the graft [5]. This dispersion may result

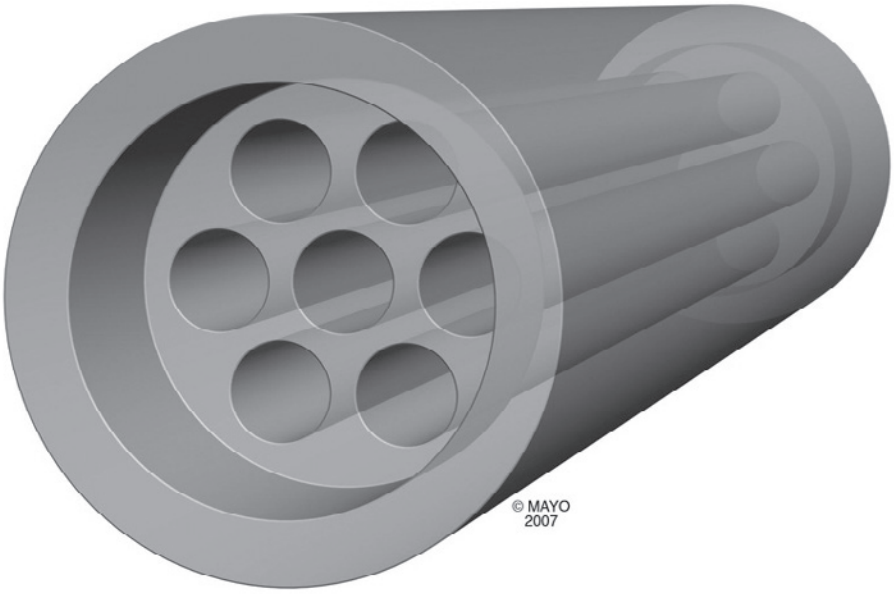

Figure 1
Drawing of a multichannel nerve tube with seven channels (400 μm in diameter) and sleeves on both ends for implantation.

in: 1) misdirection of regenerating axons, or 2) polyinnervation of different targets by dispersion of axonal branches originating from the same motoneuron. Dispersion probably occurs less after autograft repair by separate guidance of axonal branches inside the basal tubes, resulting in more grouped muscle fiber reinnervation [6]. Multichannel conduits (Figure 1), which have been developed for both experimental peripheral nerve repair [7-9] and spinal cord repair [10-12], may also limit this dispersion by separately guiding groups of regenerating axons inside the channels.

In this study, we used simultaneous and sequential tracing techniques to investigate the accuracy of motor axon regeneration across autograft, single lumen, and multichannel pol(lactic-*co*-glycolic acid) (PLGA) nerve tubes in a 1-cm gap of the rat sciatic nerve model. Simultaneous tracing of the tibial and peroneal nerves with fast blue (FB) and diamidino yellow (DY), respectively, was performed to quantify axonal dispersion for the percentage of motoneurons with double projections to both branches (Figure 2). Sequential tracing of the peroneal nerve with DY injection before repair and FB application 8 weeks after repair was used to quantify the percentage of peroneal motoneurons correctly directed to the peroneal nerve branch (Figure 3). In addition, quantitative results of regeneration were analyzed with compound muscle action potential (CMAP) recordings and nerve and muscle morphometry.

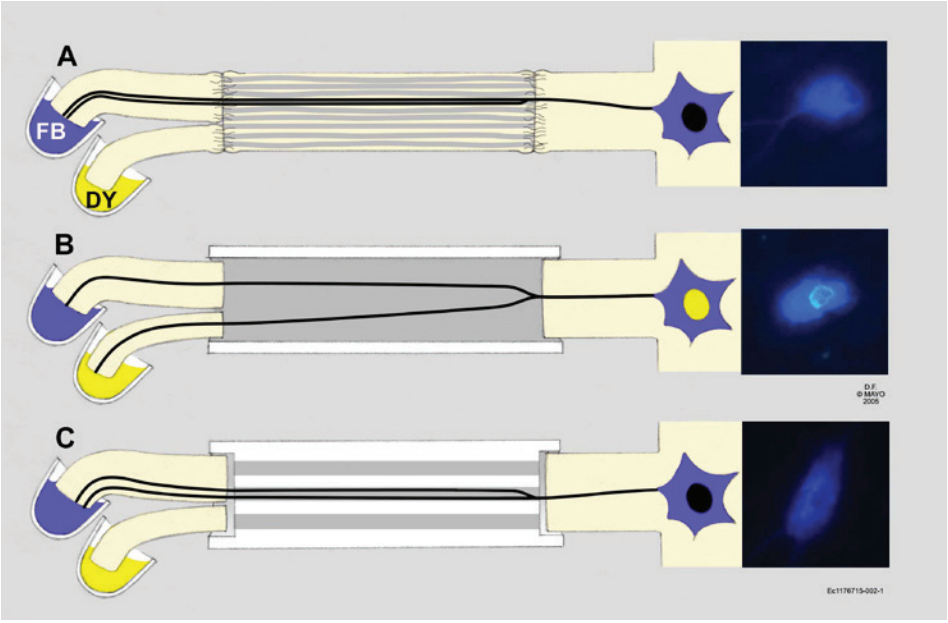

Figure 2
Technique of simultaneous retrograde tracing and concepts for the dispersion of regenerating motor axons after autograft, single lumen, and multichannel nerve tube repair. Simultaneous tracing: fast blue (FB) and diamidino yellow (DY) are applied to the tibial and peroneal nerve branches, respectively, 8 weeks after implantation. FB is transported retrograde to the cell body of the motoneuron and DY to the nucleus. A, after autograft repair, regenerating axons originating from the same motoneuron are contained by the basal lamina tubes, and both end up in the same (tibial) nerve branch. B, after single lumen nerve tube repair, axons originating from the same motoneuron disperse and end up separately in the tibial and peroneal nerve branches. C, after multi-channel nerve tube repair, axons originating from the same motoneuron are contained to the inside of a channel and end up in the same (tibial) nerve branch.

MATERIAL AND METHODS

Experimental groups

Sprague-Dawley rats weighing between 250 and 275 g were randomly assigned to one of the experimental groups for autograft (n = 17), single lumen (n = 30) or multi-channel (n = 30) (PLGA) nerve tube repair. For autograft repair, seven animals were used for simultaneous tracing, and six animals were for CMAP recording and nerve and muscle morphometry. Results for sequential tracing (n = 4) were obtained from another study [13] (**Chapter 4**). For single lumen and multichannel nerve tube repair, 12 animals were used for simultaneous tracing, 12 animals for sequential tracing, and 6 animals for CMAP recording and nerve and muscle morphometry. Control animals were included for simultaneous tracing (n = 4) and for CMAP recording and nerve and muscle morphometry (n = 4). All procedures were

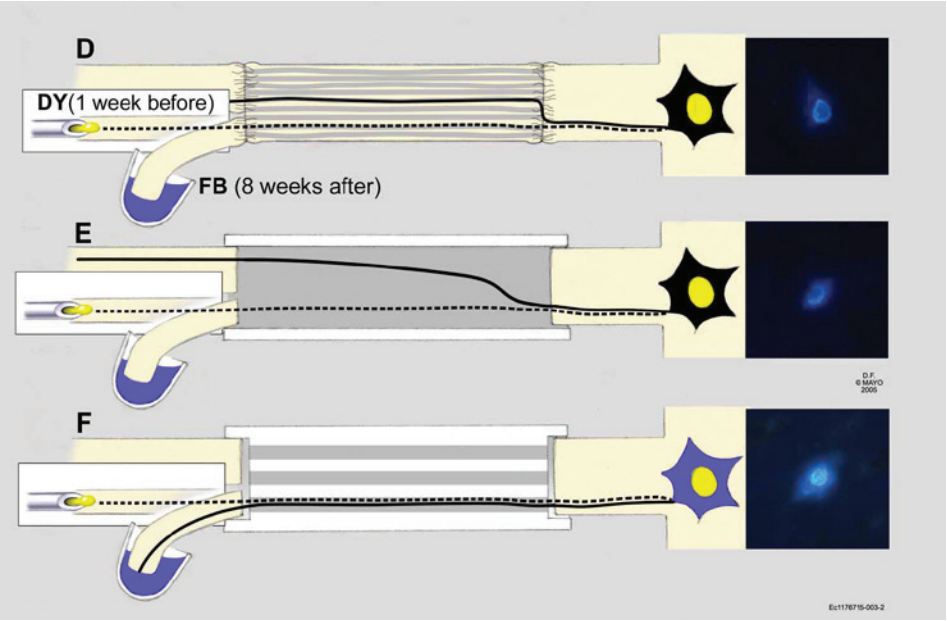

Figure 3

Technique of sequential retrograde tracing and concepts for misdirection of regenerating motor axons after autograft, single lumen, and multichannel nerve tube repair. Sequential tracing: the first tracer, DY, is injected into the peroneal nerve branch before nerve injury and is transported retrogradely to the motoneuron nucleus (dashed line). The second tracer, FB, is applied to the peroneal nerve branch 8 weeks after repair and is transported retrograde to the motoneuron cell body (continuous line). A, after autograft repair, regenerating axons are misdirected as a result of tension and/or fibrosis at the coaptation site. B, after single lumen nerve tube repair, there is no tension/fibrosis at the coaptation site, but axons may disperse. C, after multi-channel nerve tube repair, there is again no tension/fibrosis at the coaptation site and also no dispersion of regenerating axons. The dashed line illustrates the course of the original axon, and the continuous line illustrates the course of the regenerated axon form the same motoneuron.

approved by and performed according to the animal care guidelines of the Mayo Foundation Institutional Animal Care and Use Committee.

Single lumen and multichannel nerve tube fabrication

Single lumen and multichannel PLGA nerve tubes were fabricated through an injection-molding solvent evaporation technique [14] (**Chapter 6**) with the use of the same Teflon mold for the fabrication of single lumen and multichannel nerve tubes, except with different mold assemblies. The mold consisted of cylindrical spaces (2.1mm in diameter) with caps on both ends, through which either one stainless-steel wire (1.6mm in diameter), for the fabrication of single lumen nerve tubes, or seven stainless-steel wires (400μm in diameter), for the fabrication of multi-channel nerve tubes, were inserted (wires from Small Parts, Inc., Miami

Lakes, FL; mold designed and produced at Mayo Clinic). The caps for the fabrication of a multichannel nerve tube provided for an extra 1-mm sleeve on each end for implantation (Figure 1).
A solution of PLGA (copolymer ratio: lactic acid: glycolic acid, 75:25; 92kD, Fisher Scientific, Hampton, NH) in methylene chloride (300mg/450μl) was injected into the mold. The mold was placed in a vacuum for rapid solvent evaporation, thus creating a highly porous tube structure [14] (**Chapter 6**). Nerve tubes were sterilized in ethanol and pre-wetted in sterile phosphate-buffered saline before implantation.

Surgical techniques and animal care

Animals were deeply anesthetized with a mixture of ketamine (80 mg/kg) and xylazine (2.5 mg/kg), injected intraperitoneally. The sciatic nerve was exposed through a dorsal gluteal splitting approach with the aid of an operating microscope (Carl Zeiss, Inc., Oberkochen, Germany). For autograft repair, the nerve was transected at 2 sites, 1 cm apart, and immediately repaired with fascicular alignment by the use of 10-0 sutures (Ethilon; Ethicon, Inc., Piscataway, NJ; proximal 4 sutures, distal 3-4 sutures for the tibial branch and 2-3 for the peroneal branch).
For single lumen and multichannel nerve tube repair, the nerve was also transected at the same 2 sites. First, the proximal end was pulled 1mm into a 12-mm nerve tube (with a single 10-0 suture) while the original alignment was preserved; then the same procedure was performed distally for insertion of the tibial and peroneal branches separately, resulting in the creation of a 1-cm gap. Fibrin glue (Tisseel VH fibrin sealant; Baxter, Deerfield, IL) was applied to both ends of the tube to seal the lumen and sleeve. Multichannel nerve tubes were always implanted with the same orientation of the channels in relation to the nerve. The wound was closed in layers. The animals received buprenorphine hydrochloride (Reckitt Benckiser Healthcare, Slough, England) to control pain.
Postoperatively, animals were housed in individual cages with a 12-hour light-dark cycle, and water and food were available ad libitum. The operated limb was sprayed daily with Chewguard (Butler Corporation, Greensboro, NC) to prevent autotomy. A wire mesh was placed inside the cage to prevent contractures of the foot and ankle [15].

Simultaneous and sequential tracing

In the simultaneous tracing experiment, fast blue (FB) and diamidino yellow (DY) tracers (both from EMS-Chemie, Mannedorf, Switzerland) were applied to the tibial and peroneal nerve branches, respectively, 8 weeks after implantation (Figure 2). First, the tibial nerve was transected and placed in a cup containing 1.5μl of 5% FB solution for 30 minutes, followed by peroneal nerve transection and capsule application with 1.5μl of 5% DY solution for 30 minutes. The nerve ends were cleaned with 0.9% saline and sutured into surrounding fat tissue to prevent tracer leakage and cross-contamination.

In the sequential tracing experiment, 1µl of 5% DY solution was injected into the peroneal branch 1 week before implantation with the use of a scaled glass syringe (Hamilton Co., Reno, NV) with a 25-gauge needle (Figure 3). Eight weeks after implantation, the sciatic nerve was re-exposed, and the peroneal nerve was transected proximal to the previous injection site, and placed in a cup containing 1.5µl 5% FB solution for 30 minutes. Again, the nerve end was cleaned with 0.9% saline and sutured into surrounding fat tissue to prevent tracer leakage.
Animals were allowed to survive for 6 days after tracer application and then were perfused with phosphate-buffered salline and 4% paraformaldehyde and 10% sucrose. Spinal cord segments L1 to L6 were removed and post-fixed overnight. Tissue was embedded in tissue-freezing medium (Triangle Biomedical Services, Inc., Durham, NC) and stored at -80ºC until sectioning. Sagittal longitudinal 30-micron thick sections were cut on a cryostate at -20 ºC. Slides were immediately evaluated under a fluorescent microscope (Axioplan 2, Carl Zeiss, Inc. Oberkochen, Germany) with a DAPI filterset (360/400-nm bandpass excitation filter, 440-nm-long pass emission filter, and a 400nm dichroic beamsplitter) at magnification 20x with a planapochromatically corrected microscope 20x/0.75 objective (Plan Apochromat; Carl Zeiss, Inc.).
Neuronal profiles were counted in every section by one and the same observer that was blinded for the different experimental groups. Only profiles with a visible nucleus were counted. Profiles with blue cytoplasm and a dark nucleus were counted as FB-labeled, profiles with a yellow nucleus and dark cytoplasm as DY-labeled, and profiles with a yellow nucleus and blue cytoplasm as FB-DY double labeled. Profiles were counted in all sections. No corrections were made for the possibility of counting split motoneurons. Persistence of tracer in the sequential tracing experiment was analyzed from the distribution of double labeled profiles. If double labeled profiles were present in an area of the anterior horn that was normally exclusively occupied by tibial motoneurons (determined in normal animals in the simultaneous tracing experiment), the case was excluded. In the simultaneous tracing experiment, the percentage of double labeling for motoneurons with double projections was calculated by dividing the total number of double labeled profiles by the total number of labeled profiles. In the sequential tracing experiment, the percentage of correctly routed peroneal motoneurons was calculated by dividing the total number of double labeled FB-DY profiles by the total number of initially with DY labeled profiles (single labeled DY and double labeled FB-DY).

Compound muscle action potential recording

In the experiment on CMAP recording and nerve and muscle morphometry, CMAPs were recorded at 4, 6, 8, 10 and 12 weeks after implantation. CMAPs were recorded with the use of electromyography (Nicolet Viking IV; Viasys Healthcare, Inc., Conshohocken, PA) in the tibial and peroneal nerve-innervated footmuscles of the operated limb. Needle recording electrodes were placed in the plantar or dorsal footmuscles referenced to needle electrodes placed distally in the foot dig-

its. Needle-stimulating electrodes were placed directly posterior to the tibia with approximately 5 mm between the distal cathode and proximal anode. The stimulating electrodes were adjusted locally to produce the maximal CMAP amplitude. The stimulus was increased incrementally to produce a supramaximal response. CMAPs were recorded and analyzed for the amplitude, the area under the curve, and the latency of the action potential.

Nerve morphometry

The graft was reexposed 12 weeks after autograft, single lumen and multichannel nerve tube repair and fixed in situ with a 2.5% glutaraldehyde solution in phosphate-buffered saline for 30 minutes [16]. The graft was resected and placed in the same fixative overnight. Specimens (1 mm) were selected 2 mm proximal, at the mid, and 2 mm distal to the graft and embedded in spur resin for post-fixation in 1% osmium tetraoxide. Sections (1 μm) were cut with a glass knife on an ultramicrotome and stained with 1% phenylenediamine. The number of myelinated axons and mean size were analyzed at all three levels using the imaging system for nerve morphometry (Peripheral Nerve Laboratory of Dr Peter J. Dyck, Mayo Clinic Rochester). Between 500 and 600 myelinated axons were randomly selected in the slide and analyzed at 63x magnification [16].

Muscle morphometry

After resection of the graft, the soleus muscle was resected, placed in a plastic cup containing tissue-freezing medium, frozen with isopentane and liquid nitrogen, and stored at -80ºC until sectioning. Transverse 10 μm sections were cut on the cryostate at -20ºC. Sections taken from the mid-belly of the muscle were stained for myofibrillar ATPase at pH 9.4 according to the method described by Brook and Kaiser [17] staining slow (type I) fibers light and fast (type II) fibers dark. The total muscle fiber surface area was determined with an image analysis system (KS400 system, version 3.0; Zeiss, **Chapter 4**) [6]. The number of type I and type II fibers were counted. The mean muscle fiber size was calculated by dividing the total muscle fiber surface area by the total number of muscle fibers (type I and II).

Statistical analysis

Statistical analysis was performed by one-way analysis of variance with post-hoc Bonferroni tests. *P* values less than 0.05 were considered significant.

RESULTS

Number of analyzed animals per experimental group

Successful regeneration across the nerve graft (determined from the presence of FB-, DY-, or FB-DY-labeled profiles in the anterior horn after simultaneous tracing; the presence of FB-labeled profiles after sequential tracing; or the presence

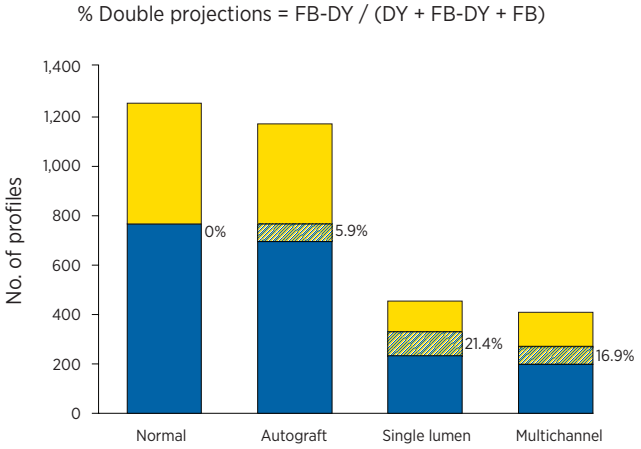

Figure 4

Bar graphs showing the results of simultaneous tracing for the mean number of FB-, DY- and FB-DY-labeled profiles and the percentages of double-projecting motoneurons in normal animals (n = 4), and after autograft repair (n = 7), single lumen (n = 4), and multichannel (n = 6) nerve tube repair. FB-labeled profiles (blue bars) represent motoneurons with exclusive projections to the tibial nerve. DY-labeled profiles (yellow bars) represent motoneurons with exclusive projections to the peroneal nerve. FB-DY-labeled profiles (striped bars) represent motoneurons with projections to both tibial and peroneal branch. No corrections were made for counting split cells (see material and methods). The percentages of double projections were calculated by dividing the number FB-DY-labeled profiles by the total number of profiles.

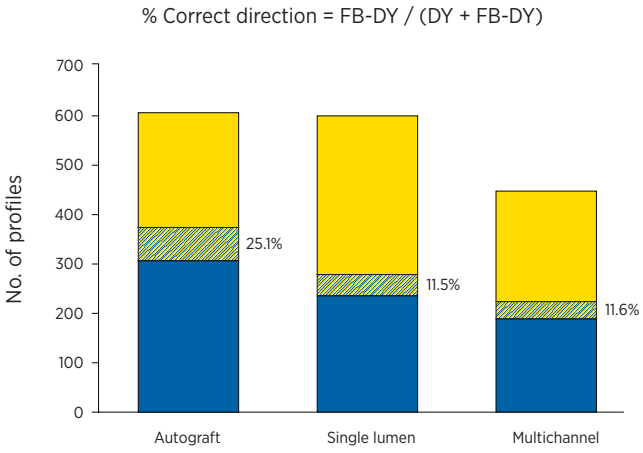

Figure 5

Bar graphs showing the results of sequential tracing for the mean number of FB-, DY-, and FB-DY-labeled profiles, and the percentages of correctly directed peroneal motoneurons after autograft (n = 4), single lumen (n = 5), and multichannel (n = 2) nerve tube repair. FB-labeled profiles (blue bars) represent misdirected tibial motoneurons. DY-labeled profiles (yellow bars) represent both misdirected and nonregenerated motoneurons. FB-DY-labeled profiles (striped bars) represent the number of correctly directed peroneal motoneurons. The percentages of correctly directed motoneurons were calculated by dividing the number of FB-DY-labeled profiles by the total number of DY-labeled profiles (DY and FB-DY).

of CMAPs and myelinated axons distal to the graft) was found in 17 (100%) of 17 animals after autograft repair, in only 16 (53.3%) of 30 animals after single lumen nerve tube repair, and in 13 (43.3%) of 30 animals after multichannel nerve tube repair. Animals that had no signs of regeneration across the nerve tube were excluded from further analysis because of the confounding effect on the results for the cases with successful regeneration (for example, including the cases with no signs of regeneration would lead to low percentages of double-projecting motoneurons because of 0% double-labeling in these cases). In addition, in the simultaneous tracing experiment, two cases of single lumen PLGA nerve tube repair were excluded from further analysis because of exclusive regeneration to the tibial branch (presence of only FB-labeled profiles). In the sequential tracing experiment, one case of single lumen nerve tube repair was excluded from further analysis because of persistence of the DY tracer, and one case of multichannel nerve tube repair was excluded because of failure to label the original peroneal motoneuron pool.

Simultaneous tracing

Spinal organization of single-labeled FB and DY profiles in control animals demonstrated that the tibial and peroneal motoneuron pool are normally present in two separate, nonintermingling spinal nuclei in the anterior horn at the levels L2 to L6. After autograft, single lumen and multichannel nerve tube repair, this spinal organization was disturbed, and FB-, DY- and FB-DY-labeled motoneurons were found intermingled.

The percentages of double projections were significantly different after autograft repair and for the cases with successful regeneration after single lumen and multichannel PLGA nerve tubes repair (F[2,14] = 16.5; P = 0.0002) (Figure 4). After single lumen nerve tube repair, more motoneurons had double projections to both the tibial and peroneal nerve branches (21.4 ± 4.9%) than after autograft repair (5.9 ± 2.9%; P-value <0.001 for posttest). The percentage after multi-channel tube was slightly lower (16.9 +/- 6.0%) compared with single lumen tube repair, but this difference was not significant. The total number of motoneurons from which axons had regenerated into in the tibial and/or peroneal nerve branch were significantly different from the normal number of motoneurons (1246 ± 43) (F[3.17] = 48.3; P < 0.0001), except after autograft repair (1140 ± 179). The total numbers after single lumen (448 ± 108) and multichannel (406 ± 156) nerve tube repair were not significantly different.

Sequential tracing

Differently labeled profiles (FB, DY, or FB-DY) were also found to be intermingled in the anterior horn after sequential tracing and autograft, single lumen, and multichannel tube repair. The size of the nucleus of profiles was variable, especially for DY profiles (ranging from 10 to 20 μm in diameter). Therefore, no corrections were made for the profiles counts based on the size of profile nucleus [18].

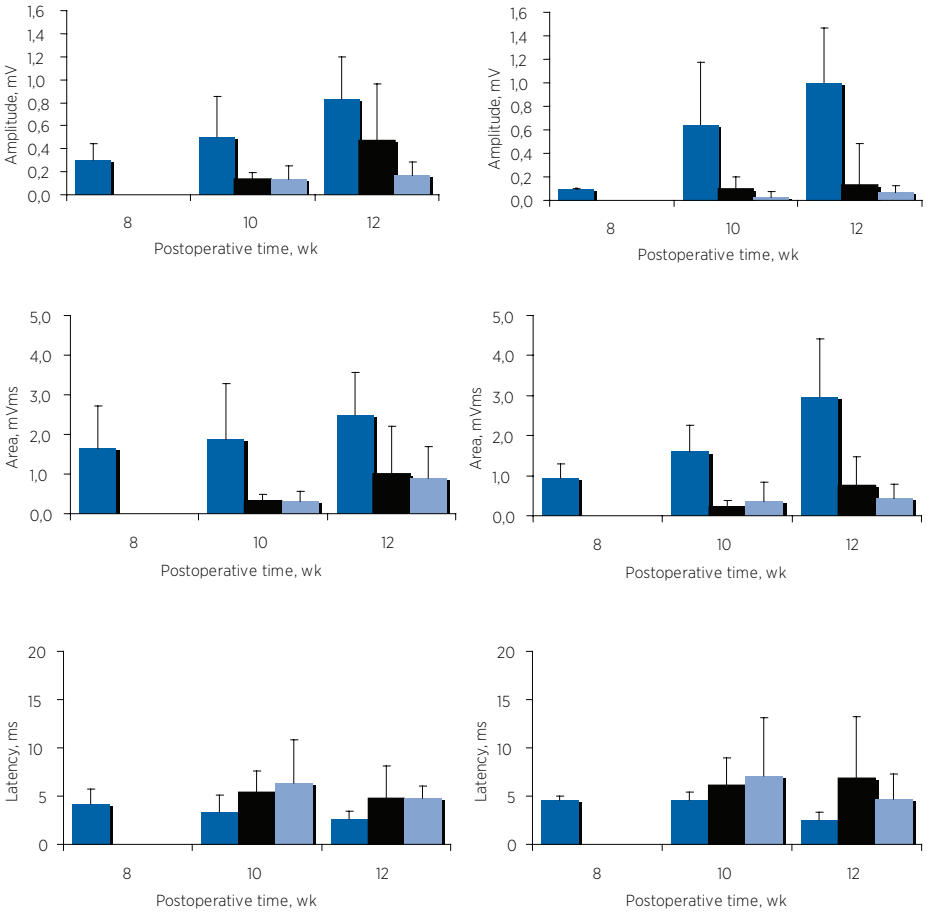

Figure 6

Results of compound muscle action potential recordings for the amplitude (A and B), area (C and D) and latency (E and F) recorded in the plantar (A, C, and E) and dorsal (B, D, and F) foot muscles 8, 10 and 12 weeks after autograft (blue), single lumen (black), and multichannel (light blue) nerve tube repair. Results are presented as means and standard deviations.

The percentages of correct direction were significantly different after autograft repair and for the cases of successful regeneration, after single lumen and multichannel PLGA nerve tube repair ($F[2,8] = 9.4$; $P = 0.008$) (Figure 5). The percentage after autograft repair (25.1 ± 6.6%) was significantly greater than with single lumen (11.5 ± 3.8%) and multichannel (11.6 ± 3.7%) nerve tubes ($P < 0.05$ for both posttests); however, these percentages were probably underestimated because of the decreased number of regenerated motoneurons after single lumen and multichannel nerve tube repair, resulting in a relatively high number of single DY-labeled

Table 1

Number and mean size of myelinated axons in normal rats, proximal to, at the middle of, and distal to the graft 12 weeks after autograft, single lumen, and multichannel nerve tube repair [a]

	Proximal to the graft		Middle of the graft		Distal to the graft	
Group	**No.**	**Size, mm**	**No.**	**Size, mm**	**No.**	**Size, mm**
Normal (*n*=4)						
mean	8,320	7.74	7,726	8.04	7,650	8.02
SD	533	0.33	378	0.39	464	0.46
Autograft repair (*n*=6)						
mean	11,958	4.66	14,459	3.43	11,578	3.74
SD	1,545	0.70	1,052	0.19	1,216	0.03
Single lumen nerve tube (*n*=4)						
mean	12,012	4.13	3,024	3.80	3,336	3.82
SD	3,404	0.63	1,094	0.34	2,205	0.04
Multichannel nerve tube (*n*=2)						
mean	10,650	3.81	2,929	4.01	3,320	4.04
SD	---[b]	---[b]	2,534	0.36	1,547	0.18

[a] SD, standard deviation.

[b] SD was incalculable because 1 sample was embedded longitudinally and therefore was lost.

profiles. After correction for the number of regenerated profiles found with simultaneous tracing, the percentages of correctly directed peroneal motoneurons are similar (27.4% for autograft, 32.0% for single lumen, and 35.6% for multichannel nerve tube repair). Considering the sizes of the peroneal and tibial motoneuron pool found with simultaneous tracing (487[39%] and 760[61%] motoneurons, respectively), theses percentages indicate that regeneration was non specific after all types of repair.

Compound muscle action potentials

The first CMAPs were detected at 8 weeks after autograft repair, compared with 10 weeks in the cases of successful regeneration after single lumen and multichannel PLGA nerve tube repair (Figure 6A and B). The CMAP amplitude and area recorded at 12 weeks were only significantly different in the dorsal foot muscles (F[2,9] = 9.7; P = 0.0057 and F[2,9] = 6.2; P = 0.0199, respectively); they were not significantly different in the plantar foot muscles (F[2,9] = 4.1; P = 0.05 and F[2,9] = 3.3; P = 0.08, respectively) (Figure 6A-D), with a significantly larger CMAP amplitude and area after autograft repair than with single lumen and multichannel nerve tube repair (P < 0.05 for both posttests, except for the comparison of the

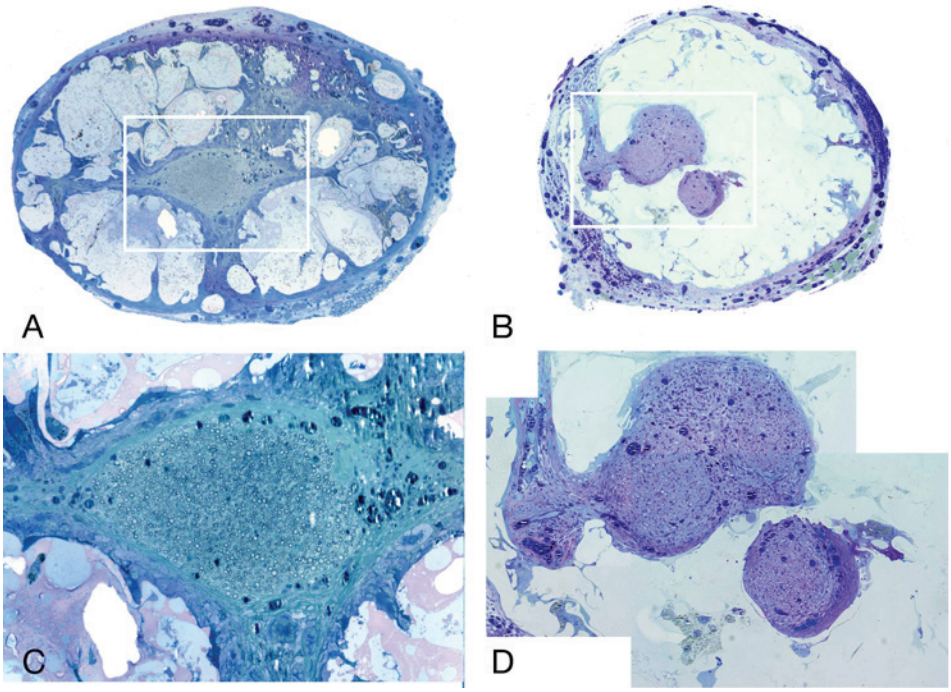

Figure 7

Microscopic sections from the middle of single lumen (A and C) and multichannel (B and D) nerve tubes 3 months after implantation. Toluidine blue for myelinated axons; original magnifications, x40 (A and B) and x160 (C and D). Note that after multichannel nerve tube repair, only 3 out of 7 channels were filled with myelinated axons. The original shape and orientation of the lumen/channels were lost, possibly because of swelling, degradation, and tapering or bundling of the channels towards the middle of the nerve tube.

CMAP area after autograft and single lumen nerve tube repair). The CMAP latency decreased with time after all repair techniques (Figure 6E and F).

Nerve morphometry

The number of myelinated axons at the midpoint and distal to the graft was significantly different from normal after autograft and after single lumen and multichannel PLGA nerve tube repair ($F[3,11] = 88.6$; $P < 0.001$ and $F[3,8] = 23.9$; $P = 0.0002$); four samples were lost because of longitudinal embedding (Table 1). After autograft repair, these numbers were significantly increased ($P < 0.001$ and $P < 0.05$, respectively). In the cases with successful regeneration after single lumen and multichannel PLGA nerve tube repair, these numbers were significantly decreased ($P < 0.001$ and $P < 0.05$ at the midpoint; and $P < 0.01$ and $P < 0.05$ distal to the graft, respectively).

Table 2

Mean muscle fiber size and distributions of type I and type II fibers in normal rats and 12 weeks after autograft, single lumen, and multichannel nerve tube repair

	Muscle morphometry	Muscle fiber types, no (%)	
Group	Mean muscle fiber size, x103 μm2	type I	type II
Normal (*n*=4)			
mean	6.60	648 (91)	69 (9)
SD	1.33	79 (4)	44 (4)
Autograft repair (*n*=5*)			
mean	4.50	307 (40)	447 (60)
SD	0.43	151 (10)	166 (10)
Single lumen nerve tube (*n*=3)			
mean	2.80	239 (40)	360 (60)
SD	0.48	22 (4)	58 (4)
Multichannel nerve tube (*n*=2)			
mean	4.00	536 (74)	197 (26)
SD	0.42	499 (1)	187 (1)

SD, standard deviation, *one soleus muscle was lost.

There was no significant difference for single lumen and multichannel PLGA nerve tube repair, despite the more than twofold smaller cross sectional lumen area available for regeneration in the multichannel nerve tube compared with the single lumen nerve tube (0.8 mm^2 for seven channels 400um in diameter, compared with 2.0 mm^2 for a single lumen nerve tube with a lumen diameter of 1.6mm), and the fact that only 3 out of 7 channels were filled with myelinated axons (Figure 7). The number of myelinated axons proximal to the graft was increased after all types of repair, although not significantly. The mean size of myelinated axons was significantly decreased compared with normal after all types of repair (proximal to the graft, $F[2,9] = 31.4$, $P < 0.0001$; mid, $F[3,11] = 190.2$, $P < 0.0001$; and distal, $F[3,8] = 257.0$, $P < 0.0001$), with no significant difference for autograft, single lumen, and multichannel nerve tube repair ($P > 0.05$ for all posttests, except for the comparison of single lumen and multichannel nerve tubes distal to the graft [$P < 0.05$]).

Muscle morphology

The number of muscle fibers was not significantly different in normal animals, after autograft, and in the cases with successful regeneration after single lumen and multichannel PLGA nerve tube repair (Table 2). The mean size of the muscle fib-

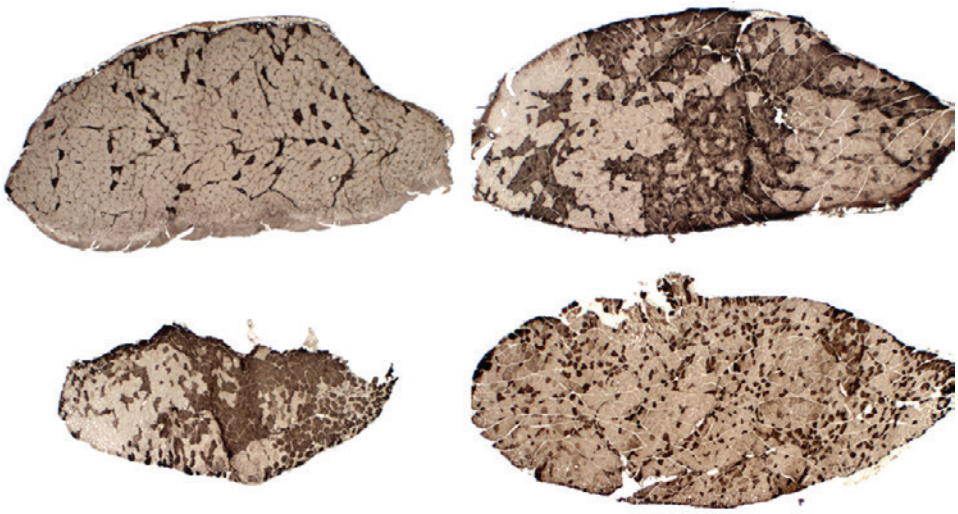

Figure 8

Microscopic sections taken from the mid-muscle belly of a normal soleus muscle (A) and after autograft repair (B), single lumen nerve tube repair (C), and multichannel nerve tube repair (D). Distribution of type I (light) and type II (dark) fibers changed from predominantly type I in normal muscle (A) to more type II than type I fibers after autograft repair (B) and single lumen nerve tube repair (C), but it was more equal to normal after multi-channel nerve tube repair (D).

ers was significantly different from normal after all types of repair (F[3,10] = 13.2; P = 0.0008), with no significant difference after autograft, single lumen, and multichannel PLGA nerve tube repair. The distribution of type I and type II muscle fibers had changed from more type I than type II in a normal soleus muscles (10:1) to more type II than type I after autograft and single lumen nerve tube repair (F[3,10] = 30.8; P < 0.0001, with P < 0.001 for both posttests) (Figure 8). For the successful cases of multichannel nerve tube repair, this distribution (3:1 ratio) was not significantly different from normal.

DISCUSSION

Accuracy of regeneration, ie, the event in which axons find their original or related end organ, is essential to obtain functional recovery when a nerve gap has to be bridged. Autografts are routinely used. In recent years, different single lumen nerve tubes have been introduced to serve as guidance for axonal outgrowth [1]. Little is known about the potential effect of single lumen nerve tube structure on the accuracy of regeneration as compared with the autograft [6], and even less is known about the effect of more complex structures, such as the multichannel nerve tube. In this study, we used simultaneous and sequential retrograde tracing techniques to compare the accuracy of motor axon regeneration across autograft,

single lumen and multichannel PLGA nerve tube repair in a 1-cm gap of the rat sciatic nerve model.

Single lumen nerve tube versus autograft repair

Simultaneous tracing in our study showed increased dispersion of regenerating axons in the cases in which there was successful regeneration across the single lumen nerve tube, with more double projecting motoneurons (21.4%) than after autograft repair (5.9%). Sequential tracing showed no difference in the direction of regenerating axons, with similar percentages of correctly directed peroneal motoneurons (after correction for the decreased number of regenerated profiles). Although various methods have been used to investigate the accuracy of reinnervation after single lumen nerve tube repair [19-23], this is, to our knowledge, the first study that compares the accuracy of regeneration across single lumen nerve tubes and autografts using simultaneous and sequential tracing.

Technical note

Numerous factors have to be considered in the interpretation of our results from tracing, including the size of the nerve gap, time point of evaluation, technique of tracing, and physical properties of the nerve tube. Dispersion has been found to increase with gap length [5]. Also, the number of double-projecting motoneurons has been found to decrease again with time [24]. Axonal branching with polyinnervation, followed by pruning, may therefore actually be a mechanism to correct for misdirection. This can explain the lower percentages of multiple-projecting motoneurons that were found by Valero-Cabré et al. 90 days after repair of 8-mm nerve gaps with single lumen poly-L-lactid-ε-caprolactone (6.0%) and silicone nerve tubes (10%) (compared with 5.6% after autograft repair) [22]. More research is needed to further investigate the influence of nerve gap size and the effect of the time point of evaluation in the analysis of the accuracy of regeneration across nerve tubes.

Factors concerning the techniques of tracing must also be considered. In this study, we used FB and DY tracers for both simultaneous and sequential tracing. This combination of tracers has been investigated in detail by Puigdellivol-Sánchez et al. [25-27]. The practical advantage of this technique is that both tracers can be visualized with the same filter. The sequential tracing technique with DY injection followed by FB application 8 weeks after repair has a high labeling efficiency (86.9% Puigdellivol et al. [25] and 91.3% **Chapter 4**) that is higher than the technique of tracer muscle injection [28], which has been used previously to investigate the accuracy of muscle reinnervation after nerve tube repair [19, 21]. There is also no significant fading of the first tracer (DY) or blockage of uptake of the second one (FB) [27]. Problems of the nerve injection technique, however, are: 1) persistence of DY tracer that may lead to overestimation of the percentage correctly directed motoneurons [26], and 2) damage to the nerve before nerve injury and repair that may affect regeneration to the peroneal nerve branch. In our study, only

one case of significant persistence of tracer was found. The number of motoneurons from which axons had regenerated into the peroneal branch did not appear to be different after simultaneous and sequential tracing (compare the number of DY- plus FB-DY-labeled motoneurons in Figure 5). In addition, the size of the nerve used for sequential tracing must be considered. Recently, Puigdellivol-Sánchez et al. [29] found a much higher percentage of correctly directed tibial motoneurons after direct coaptation repair (87%) by using the same technique and time point of evaluation. The difference with our results might be explained by the difference in repair techniques (direct coaptation vs graft repair [13], **Chapter 3**) and by the larger size of the tibial motoneuron pool.

Different physical properties of the nerve tube may also affect results. In our study, nerve tubes were made of PLGA using an injection-molding solvent evaporation technique [14] (**Chapter 6**). This biomaterial has been approved by the United States Food and Drug Administration (FDA); is biodegradable, biocompatible, and sterilizable; can be used for sustained-release drug delivery; and has been used previously to fabricate both single lumen and multichannel nerve tubes [8, 30, 31]. We recently found in vitro, however, that PLGA nerve tubes swell extensively, especially for lower lactic acid-to-glycolic acid ratios [14] (**Chapter 6**). Swelling may block the lumen or channels for regeneration or compress regenerated axons. In addition, acidic products formed during the degradation process may interfere with regeneration, and PLGA nerve tubes may elongate and collapse [30, 32]. These factors can explain the disappointing results found after PLGA nerve tube repair in our study, with successful regeneration across the nerve tube in only approximately 50% of the cases and, in these cases, with significantly decreased numbers of motoneurons from which axons had regenerated across the nerve tube, compared with normal and autograft repair.

Currently, we are investigating the use of novel biomaterials, for example, poly(caprolactone fumarate), which self-cross-links and can, therefore, also be used for the injection-molding technique of fabrication [33]. Another physical property that may affect the accuracy of regeneration is the permeability of the nerve tube, which may control the exchange of external and internal neurotrophic factors and molecules involved in the formation of the fibrin matrix inside the nerve tube [23]. Both single lumen and multichannel PLGA nerve tubes used in this study were highly permeable because of the solvent evaporation technique of fabrication [14] (**Chapter 6**).

Finally, it must be noted that we used an optimized technique for autografting with an immediate direct repair of matched size nerve stumps in this study. Results might differ from clinical nerve repair with interposition of multiple sural nerve grafts after a time delay. Moreover, in clinical nerve repair, it is not always possible to accurately determine and reconstruct the fascicular architecture of the nerve.

Although different factors must thus be considered in the interpretation of results, our study demonstrates that simultaneous and sequential tracing techniques provide new insights into the accuracy of regeneration across nerve tubes. Of course,

conventional evaluation methods (including CMAP recording and nerve and muscle morphometry) and functional analysis will still have to be performed, especially in the development of a nerve tube for possible clinical application.

Single lumen versus multi-channel nerve tube repair

To reduce dispersion, we designed a multichannel nerve tube and compared it with a single lumen nerve tube made of the same material using the same fabrication technique. Ih this study, no significant difference between single lumen and multichannel PGLA nerve tubes were found. In our opinion, however, the concept of a multichannel nerve tube that might limit dispersion remains appealing for the following reasons.

The only slight reduction in dispersion after multichannel nerve tube repair in this study might be explained by the findings that: 1) some axons had probably already branches before entering the channel (as can be concluded from the increased number of axons proximal to the nerve graft); 2) results for the number of axons FB- and DY-labeled profiles were variable (in some cases, even exclusive regeneration to the tibial branch was found); and 3) only three of seven channels were filled with myelinated axons 3 months after multichannel PLGA nerve tube repair (compared with the large number of basal lamina tubes in an autograft, approximately 1000 in the sciatic nerve in mice) [34]. Different modifications to the multichannel nerve tube, including more channels and different channel fillings, might further reduce dispersion. A total of seven channels (400 μm in diameter) was the maximum number that fit into a tube with a 1.6-mm inner diameter, because of the minimal distance of 100 μm needed to drill holes in the end caps through which wires were inserted. Currently, we are investigating the use of 3D-printing. With this fabrication technique, nerve tubes with any shape can be built in a layer-by-layer fashion. In the future, it might even be possible with this technique to reconstruct the fascicular architecture of the nerve, which often does not consist of longitudinally aligned fascicles, but instead forms an intraneural plexus [35].

Different channel fillings, including surface coatings, growth factors, and Schwann cells, may increase both the number of axons that regenerate and the number of channels across which axons regenerate. An additional advantage of the multichannel nerve tube, therefore, is that it provides more luminal surface area than single lumen nerve tubes for cell attachment and local release of incorporated growth factors. The finding that quantitative results of regeneration in this study were similar to repair with empty single lumen and multichannel nerve tubes (despite the more than twofold smaller cross sectional lumen area for multichannel nerve tubes) encourages us to investigate further the use of different channel fillings, including neurotrophic factors that might also be of interest to guide regenerating axons, which often wander at the suture site [36], straight into the channels [37].

Finally, of interest in this study was the distribution of type I and type II fibers that was closer to normal (10:1) after multi-channel tube repair (3:1) than after both single lumen tube and autograft repair (both 2:3) (Figure 8). Although this may be

explained by various factors, it may indicate more accurate muscle reinnervation after multichannel nerve tube repair. Both the small slow soleus muscle and large fast gastrocnemic muscle [38] are innervated by the lateral gastrocnemic nerve [39] and after nerve injury and repair, the fiber type distribution in soleus muscle may change as a result of misdirection [19, 40, 41]. Despite similar changes of correct direction, multichannel nerve tube repair may therefore lead to improved muscle reinnervation, for example, by a more organized distribution of regenerated motoneurons in the anterior horn. In the present study, differences in spinal organization could not be analyzed because of the small number of regenerated profiles. More research is needed to investigate this finding further.

CONCLUSIONS

Retrograde tracing in this study demonstrated the importance of investigating the accuracy of motor axon regeneration in the development of a nerve tube for motor nerve repair. We also presented the concept of the multichannel nerve tube that might limit dispersion, although in this study no statistical difference in accuracy of regeneration across single lumen and multichannel nerve tubes was found.

ACKNOWLEDGEMENTS

We thank LouAnn Gross for advice on embedding and staining techniques, Dr. Peter J. Dyck and JaNean Engelstad for advice on nerve morphometry, and Tony Koch for excellent animal care. Baxter Healthcare Corp., Westlake Village CA, provided the fibrin glue.

REFERENCES:

1. Schlosshauer, B., et al., *Synthetic nerve guide implants in humans: a comprehensive survey.* Neurosurgery, 2006. **59**(4): p. 740-7; discussion 747-8.
2. Weber, R.A., et al., *A randomized prospective study of polyglycolic acid conduits for digital nerve reconstruction in humans.* Plast Reconstr Surg, 2000. **106**(5): p. 1036-45; discussion 1046-8.
3. Ducic, I., C.T. Maloney, Jr., and A.L. Dellon, *Reconstruction of the spinal accessory nerve with autograft or neurotube? Two case reports.* J Reconstr Microsurg, 2005. **21**(1): p. 29-33; discussion 34.
4. Navissano, M., et al., *Neurotube for facial nerve repair.* Microsurgery, 2005. **25**(4): p. 268-71.
5. Brushart, T.M., et al., *Joseph H. Boyes Award. Dispersion of regenerating axons across enclosed neural gaps.* J Hand Surg [Am], 1995. **20**(4): p. 557-64.

6. Vleggeert-Lankamp, C.L., et al., *Type grouping in skeletal muscles after experimental reinnervation: another explanation.* Eur J Neurosci, 2005. **21**(5): p. 1249-56.
7. Bender, M.D., et al., *Multi-channeled biodegradable polymer/CultiSpher composite nerve guides.* Biomaterials, 2004. **25**(7-8): p. 1269-78.
8. Sundback, C., et al., *Manufacture of porous polymer nerve conduits by a novel low-pressure injection molding process.* Biomaterials, 2003. **24**(5): p. 819-30.
9. Yang, Y., et al., *Neurotrophin releasing single and multiple lumen nerve conduits.* J Control Release, 2005. **104**(3): p. 433-46.
10. Friedman, J.A., et al., *Biodegradable polymer grafts for surgical repair of the injured spinal cord.* Neurosurgery, 2002. **51**(3): p. 742-51; discussion 751-2.
11. Moore, M.J., et al., *Multiple-channel scaffolds to promote spinal cord axon regeneration.* Biomaterials, 2006. **27**(3): p. 419-29.
12. Stokols, S. and M.H. Tuszynski, *The fabrication and characterization of linearly oriented nerve guidance scaffolds for spinal cord injury.* Biomaterials, 2004. **25**(27): p. 5839-46.
13. de Ruiter, G.C., et al., *Misdirection of regenerating motor axons after nerve injury and repair in the rat sciatic nerve model.* Exp Neurol, 2008. **211**(2): p. 339-50.
14. de Ruiter, G.C., et al., *Methods for in vitro characterization of multichannel nerve tubes.* J Biomed Mater Res A, 2008. **84**(3): p. 643-51.
15. Strasberg, S.R., et al., *Wire mesh as a post-operative physiotherapy assistive device following peripheral nerve graft repair in the rat.* J Peripher Nerv Syst, 1996. **1**(1): p. 73-6.
16. Dyck, P.J., D. P.J.B., and J.K. Engelstad, *Pathologic alterations of nerves*. Peripheral Neuropathy, ed. D. P. and T. P.K. Vol. 1. 2005, Philadelphia: Elsevier. 733-829.
17. Brooke, M.H. and K.K. Kaiser, *Some comments on the histochemical characeterization of muscle adenosine triphosphate.* J Histoechem Cytochem, 1969. **17**: p. 431-432.
18. Abercrombie, M., *Estimation of nuclear population from microtome sections.* Anat Rec, 1946. **94**: p. 239-247.
19. Bodine-Fowler, S.C., et al., *Inaccurate projection of rat soleus motoneurons: a comparison of nerve repair techniques.* Muscle Nerve, 1997. **20**(1): p. 29-37.
20. Evans, P.J., et al., *Selective reinnervation: a comparison of recovery following microsuture and conduit nerve repair.* Brain Res, 1991. **559**(2): p. 315-21.
21. Rende, M., et al., *Accuracy of reinnervation by peripheral nerve axons regenerating across a 10-mm gap within an impermeable chamber.* Exp Neurol, 1991. **111**(3): p. 332-9.
22. Valero-Cabre, A., et al., *Superior muscle reinnervation after autologous nerve graft or poly-L-lactide-epsilon-caprolactone (PLC) tube implantation in comparison to silicone tube repair.* J Neurosci Res, 2001. **63**(2): p. 214-23.
23. Zhao, Q., et al., *Specificity of muscle reinnervation following repair of the transected sciatic nerve. A comparative study of different repair techniques in the rat.* J Hand Surg [Br], 1992. **17**(3): p. 257-61.
24. Hennig, R. and E. Dietrichs, *Transient reinnervation of antagonistic muscles*

by the same motoneuron. Exp Neurol, 1994. **130**(2): p. 331-6.
25. Puigdellivol-Sanchez, A., et al., *Fast blue and diamidino yellow as retrograde tracers in peripheral nerves: efficacy of combined nerve injection and capsule application to transected nerves in the adult rat.* J Neurosci Methods, 2000. **95**(2): p. 103-10.
26. Puigdellivol-Sanchez, A., et al., *Persistence of tracer in the application site--a potential confounding factor in nerve regeneration studies.* J Neurosci Methods, 2003. **127**(1): p. 105-10.
27. Puigdellivol-Sanchez, A., et al., *On the use of fast blue, fluoro-gold and diamidino yellow for retrograde tracing after peripheral nerve injury: uptake, fading, dye interactions, and toxicity.* J Neurosci Methods, 2002. **115**(2): p. 115-27.
28. Haase, P. and J.N. Payne, *Comparison of the efficiencies of true blue and diamidino yellow as retrograde tracers in the peripheral motor system.* J Neurosci Methods, 1990. **35**(2): p. 175-83.
29. Puigdellivol-Sanchez, A., A. Prats-Galino, and C. Molander, *Estimations of topographically correct regeneration to nerve branches and skin after peripheral nerve injury and repair.* Brain Res, 2006.
30. Evans, G.B., K. Widmer, M. Gürlek, A. Savel, T. Gupta, P. Lohman, R. Williams, J. Hodges, J. Nabawi, A. Patrick, C. Mikos, AG., *Tissue engineered conduits: the use of biodegradable poly-DL-lactic-co-glycolic acid (PLGA) scaffolds in peripheral nerve regeneration.* Biological matrices and tissue reconstruction., ed. H.R. Stark GE, Tanczos E. 1998, Berlin: Springer. 225-35.
31. Widmer, M.S., et al., *Manufacture of porous biodegradable polymer conduits by an extrusion process for guided tissue regeneration.* Biomaterials, 1998. **19**(21): p. 1945-55.
32. Evans, G.R., et al., *In vivo evaluation of poly(L-lactic acid) porous conduits for peripheral nerve regeneration.* Biomaterials, 1999. **20**(12): p. 1109-15.
33. Jabbari, E., et al., *Synthesis, material properties, and biocompatibility of a novel self-cross-linkable poly(caprolactone fumarate) as an injectable tissue engineering scaffold.* Biomacromolecules, 2005. **6**(5): p. 2503-11.
34. Giannini, C. and P.J. Dyck, *The fate of Schwann cell basement membranes in permanently transected nerves.* J Neuropathol Exp Neurol, 1990. **49**(6): p. 550-63.
35. Sunderland, S., *Nerve injuries and their repair: A critical appraisal.* . 1991, Melbourne: Churchill Livingstone.
36. Witzel, C., C. Rohde, and T.M. Brushart, *Pathway sampling by regenerating peripheral axons.* J Comp Neurol, 2005. **485**(3): p. 183-90.
37. Moore, K., M. MacSween, and M. Shoichet, *Immobilized concentration gradients of neurotrophic factors guide neurite outgrowth of primary neurons in macroporous scaffolds.* Tissue Eng, 2006. **12**(2): p. 267-78.
38. Young, B.L., et al., *An effective sleeving technique in nerve repair.* J Neurosci Methods, 1984. **10**(1): p. 51-8.
39. Gillespie, M.J., T. Gordon, and P.R. Murphy, *Reinnervation of the lateral gastrocnemius and soleus muscles in the rat by their common nerve.* J Physiol, 1986. **372**: p. 485-500.

40. Gillespie, M.J., T. Gordon, and P.R. Murphy, *Motor units and histochemistry in rat lateral gastrocnemius and soleus muscles: evidence for dissociation of physiological and histochemical properties after reinnervation.* J Neurophysiol, 1987. **57**(4): p. 921-37.
41. Ijkema-Paassen, J., M.F. Meek, and A. Gramsbergen, *Muscle differentiation after sciatic nerve transection and reinnervation in adult rats.* Ann Anat, 2001. **183**(4): p. 369-77.